Doping Dependence of an n-Type Cuprate Superconductor Investigated by Angle-Resolved Photoemission Spectroscopy

N. P. Armitage, F. Ronning, D. H. Lu, C. Kim, A. Damascelli, K. M. Shen, D. L. Feng, H. Eisaki, and Z.-X. Shen
Department of Physics, Applied Physics and Stanford Synchrotron Radiation Laboratory, Stanford University, Stanford, California 94305

P. K. Mang, N. Kaneko, and M. Greven
Department of Applied Physics and Stanford Synchrotron Radiation Laboratory, Stanford University, Stanford, California 94305

Y. Onose, Y. Taguchi, and Y. Tokura
Department of Applied Physics, The University of Tokyo, Tokyo 113-8656, Japan
(Received 20 November 2001; published 5 June 2002)

We present an angle-resolved photoemission doping dependence study of the n-type cuprate superconductor $Nd_{2-x}Ce_xCuO_{4\pm\delta}$, from the half-filled Mott insulator to the $T_c = 24$ K superconductor. In Nd_2CuO_4, we reveal the charge-transfer band for the first time. As electrons are doped into the system, this feature's intensity decreases with the concomitant formation of near-E_F spectral weight. At low doping, the Fermi surface is an electron-pocket (with volume $\sim x$) centered at $(\pi, 0)$. Further doping leads to the creation of a new holelike Fermi surface (volume $\sim 1 + x$) centered at (π, π). These findings shed light on the Mott gap, its doping evolution, as well as the anomalous transport properties of the n-type cuprates.

DOI: 10.1103/PhysRevLett.88.257001 PACS numbers: 79.60.Bm, 73.21.–b, 74.72.–h

The parent compounds of the high-temperature superconductors are believed to belong to a class of materials known as Mott insulators [1]. At half filling these materials, predicted to be metallic by band theory, are insulating due to the large Coulomb repulsion that inhibits double site occupation and hence charge conduction. These cuprates become metals and then superconductors when doped with charge carriers away from half filling. Although the general systematics of Mott insulators and metals are understood, the question of how one may proceed from a half-filled Mott insulator (with only spin low-energy degrees of freedom) to a metal (with a large Luttinger's theorem respecting Fermi surface) is unanswered. Even after 15 years of intensive research into this fundamental issue in the cuprates, both the manner in which this evolution occurs and the nature of electronic states at the chemical potential remains unclear.

Within the Hubbard model, Mott insulators are described as a single metallic band split into upper (UHB) and lower Hubbard bands (LHB) by a correlation energy U that represents the energy cost for a site to be doubly occupied. The high-T_c parent compounds are not Mott insulators *per se* but may be more properly characterized as charge transfer insulators [2]. However, it is believed that such systems can be described by an effective Hubbard Hamiltonian, where an oxygen-derived charge transfer band (CTB) substitutes for the LHB and the charge transfer gap Δ plays the role of U. Angle-resolved photoemission (ARPES) measurements on the prototypical half-filled parent Mott insulators $Sr_2CuO_2Cl_2$ (SCOC) and $Ca_2CuO_2Cl_2$ (CCOC) have shed light on the dispersive behavior of this CTB [3,4]. Interestingly, previous photoemission measurements on undoped Nd_2CuO_4 (NCO) did not reveal a similar feature [5]. This is surprising as one might expect that the half-filled CuO_2 planes would exhibit generalities independent of material class. The CTB in NCO may not have been resolved previously due to an anomalous (and yet to be understood) polarization dependence of its intensity, and because it is partially obscured by the main valence band [6].

In the simplest picture, the chemical potential moves into the LHB or UHB (with a transfer of spectral weight across the correlation gap $\sim U$ [7]), as the material is doped away from half filling with holes or electrons, respectively. In alternative scenarios, the act of doping creates "states" inside the insulator's gap, and as a result the chemical potential remains relatively fixed in the middle of the gap [8,9]. A definitive resolution of this issue has been hampered by the lack of reliable inverse photoemission experiments, that coupled with photoemission could show where the E_F states reside with respect to the CTB and UHB. Information obtained from photoemission alone on different material classes has been interpreted in terms of both scenarios [8–10].

The vast majority of ARPES experiments on the high-temperature superconductors have been performed on hole-doped materials [11,12]. In contrast, the electron-doped materials have been relatively unexplored with this technique [8,13–15]. In addition to having interesting properties of their own, these materials provide a unique opportunity to explore the evolution from a Mott insulator to a metal since a greater portion of the states should be

 © 2002 The American Physical Society

occupied making a full view of the Mott gap possible for photoemission experiments.

In this Letter, we report results of an ARPES study of the electron-doped cuprate superconductor $Nd_{2-x}Ce_xCuO_{4\pm\delta}$ at concentrations $x = 0$, 0.04, 0.10, and 0.15. For the first time, we are able to isolate and resolve the contribution to the spectra from the CTB on the $x = 0$ sample, as has been observed in the parent compounds of the hole-doped materials, thereby demonstrating the universality of the electronic structure of the CuO_2 plane. In NCO this feature appears ~1.3 eV below the Fermi energy, rendering almost the entire Mott gap visible in our experiment. Upon doping, spectral weight is shifted from the CTB to form states near E_F. At very low doping, these states are centered around $(\pi, 0)$, forming a small Fermi surface with volume $\sim x$. Simultaneously, there is an appearance of spectral weight that begins to span and fill the insulator's gap. At high doping levels, this in-gap spectral weight moves to E_F near $(\pi/2, \pi/2)$ and thereby connects with $(\pi, 0)$ derived states to form an local density approximation (LDA)-like Fermi surface with volume $\sim 1 + x$. This evolution provides a natural explanation for the confusing transport data from electron-doped cuprates and is qualitatively similar to what one expects from some $t - t' - t'' - U$ models.

Single crystals of $Nd_{2-x}Ce_xCuO_{4\pm\delta}$ (NCCO) with concentrations $x = 0$, 0.04, 0.10, and 0.15 were grown by the traveling-solvent floating-zone method in 4 atm of O_2 at Stanford University ($x = 0.04$, 0.10, and 0.15) and at The University of Tokyo ($x = 0$ and 0.15). Samples of $x = 0$, 0.10, and 0.15 were oxygen reduced. In addition some data were taken on reduced $x = 0.04$ samples and were found to have features intermediate to unreduced $x = 0.04$ and reduced $x = 0.10$. Measurements were performed at the Stanford Synchrotron Radiation Laboratory's Beam line 5-4. The data reported here were collected with 16.5 eV photons with 10–20 meV energy resolution and an angular resolution as good as 0.25° (~1% of the Brillouin zone) except where indicated. The chamber pressure was lower than 4×10^{-11} torr. In all measurements, sample temperatures were uniformly 10–20 K. This presented no charging problems even for the $x = 0$ insulator. Cleaving the samples *in situ* at 10 K resulted in shiny flat surfaces, which LEED revealed to be clean and well ordered with the same symmetry as the bulk [14,15]. No signs of surface aging were seen for the duration of the experiments (~24 h).

In Figs. 1(a) and 1(b), we show spectra for undoped NCO with polarization of the incoming photons at 45° to the Cu-O bonds. Along the Γ to the (π, π) cut, a large broad feature disperses out from under the main valence band, reaches a maximum near $(\pi/2, \pi/2)$, and then disperses back to higher energy. A very similar dispersion can be seen in the perpendicular direction [Fig. 1(b)]. A feature with a strikingly similar shape and energy scale has been seen in CCOC, as shown in Figs. 1(c) and 1(d). Because of this similarity, as well as the fact that the feature's position relative to the chemical potential (~1.3 eV; minimum binding energy of its centroid) is approximately the same as this material's optical gap ~1.6 eV (measured from the peak in the optical conductivity) [16], we assign this feature to the CTB. This assertion is supported below by its dramatic doping dependence. There is some variability (±0.1 eV) in the exact binding energy of the CTB from cleave to cleave, as also observed in CCOC and SCOC. In Figs. 1(a) and 1(b), the horizontal scale is set to the average position from a number of cleaves. In Figs. 1(c) and 1(d), the energy is given relative to the binding energy minimum of the feature. The $x = 0$ sample is probably slightly doped so that the chemical potential is pinned near the conduction band minimum (UHB). Part of the discrepancy between photoemission (~1.3 eV) and optics (~1.6 eV) may stem from the fact that the charge transfer (CT) gap appears to be indirect, as we will show later.

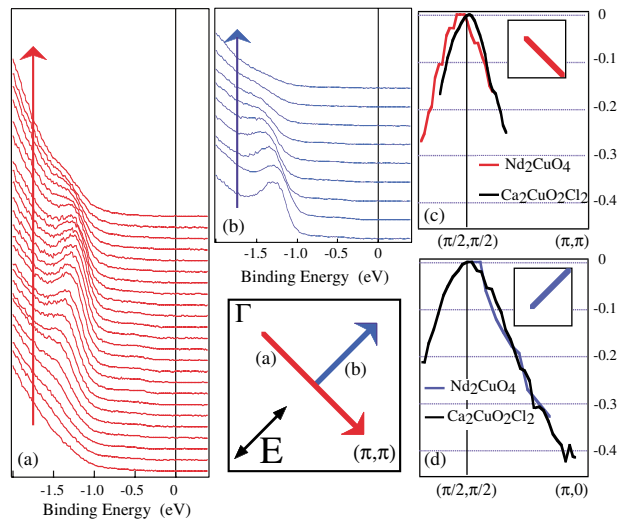

FIG. 1 (color). (a) Dispersion of the charge transfer band in Nd_2CuO_4 along zone diagonal from 25% to 75% of Γ to (π, π) distance. (b) Dispersion of the CTB from $(\pi/2, \pi/2)$ to 50% of the $(\pi/2, \pi/2)$ to $(\pi, 0)$ distance (c) and (d). Comparison of the CTB dispersion in NCO (red and blue) and CCOC (black).

Having identified the CTB in Nd_2CuO_4, we can track it as the dopant concentration is increased and spectral weight appears in the near-E_F region. In Figs. 2(a) and 2(b), we plot partially angle-integrated energy distribution curves (EDCs) from regions near $(\pi/2, \pi/2)$ and $(\pi, 0.3\pi)$, respectively. One can see that at finite doping levels the CTB spectral weight decreases and intensity develops at energies near E_F, at what is ostensibly the edge of the upper Hubbard band. This is suggestive of the kind of transfer of spectral weight from high energies to low energies that one qualitatively expects when doping a Mott insulator [7], and it gives us confidence in our assignment of this feature as the CTB.

A closer look at Fig. 2(a) reveals that there is a very weak low-energy "foot" in the $x = 0$ sample that probably reflects a small intrinsic doping level in this otherwise half-filled material. The larger nondispersive near-E_F

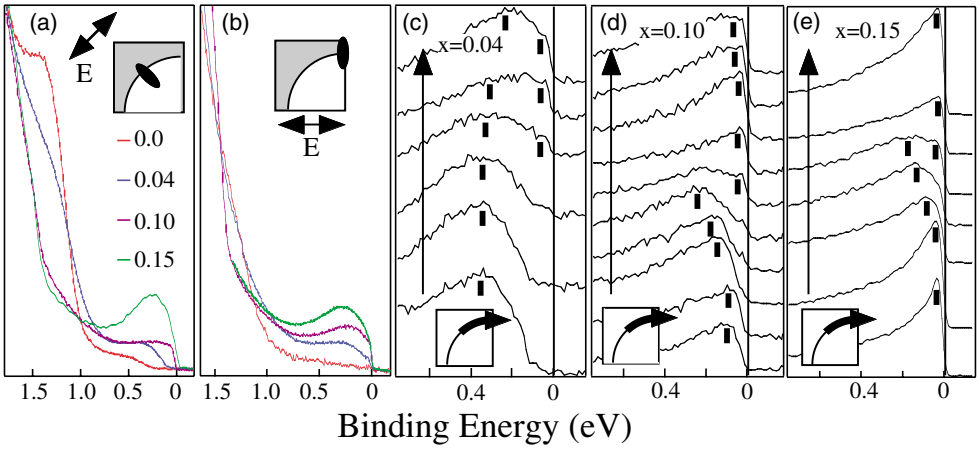

FIG. 2 (color). (a) EDCs integrated in a region near the $(\pi/2, \pi/2)$ position. (b) EDCs integrated in a region near the $(\pi, 0.3\pi)$ position. (c), (d), and (e) EDCs from around the putative LDA Fermi surface for $x = 0.04$, 0.10, and 0.15 samples, respectively.

spectral weight that develops along the zone diagonal for the $x = 0.04$ sample is gapped by $\sim$150 meV. This is in contrast to near $(\pi, 0.3\pi)$ [Fig. 2(b)], where there is spectral weight at E_F for $x = 0.04$ doping levels. For $x = 0.10$, the zone diagonal spectral weight has moved closer to E_F and even stronger E_F intensity has formed near $(\pi, 0.3\pi)$. A weak dispersion is evident along the zone diagonal for the $x = 0.10$ sample (not shown). At $x = 0.15$ there is large near-E_F weight and a strong dispersion throughout the zone as detailed in our previous work [14,15]. The small chemical potential shift ($\sim$150 meV) seen by x-ray photoemission spectroscopy in NCCO by Harima *et al.* [17] in this doping range is consistent with our result where it appears that the band at $(\pi, 0)$ moves on order of this amount when doping from $x = 0$ to $x = 0.15$.

Following our previous analysis of the optimally doped compound [14], we construct Fermi surfaces by integrating EDCs in a small window about E_F (-40 meV, $+20$ meV) and plotting this quantity as a function of $\vec{k}$ (Fig. 3). Consistent with the above observation that spectral weight along the zone diagonal is gapped for $x = 0.04$, one can see that it is only the states at $(\pi, 0)$ that can contribute to low-energy properties. Here, a Fermi "patch" indicates that there is an extremely low-energy shallow band in this part of the Brillouin zone. At $x = 0.10$, weight at E_F with low intensity begins to appear near the zone diagonal. Near $(\pi, 0)$, the "band" becomes deeper and the Fermi patch becomes a Fermi surface. At $x = 0.15$, the zone diagonal region has become intense. The full Fermi surface has formed and only in the intensity-suppressed regions near $(0.65\pi, 0.3\pi)$ (and its symmetry-related points) at the intersection of the Fermi surface with the antiferromagnetic Brillouin zone boundary does the underlying Fermi surface retain its anomalous properties [14].

We can gain more insight by looking at plots of the EDCs around the putative LDA Fermi surface, as shown in Figs. 2(c)–2(e). In Fig. 2(c), for $x = 0.04$, a large broad feature is gapped by $\sim$150 meV near the zone-diagonal region. As one proceeds around the ostensible LDA Fermi surface, the high-energy feature loses spectral weight and may disappear, while another feature pushes up at E_F. It is this second component that contacts E_F near $(\pi, 0.3\pi)$ to form the small Fermi surface (FS) for the $x = 0.04$ sample. Similar behavior is seen in the $x = 0.10$ and 0.15 plots; the lowest-energy features become progressively sharper, closer to and upon entering the metallic state. The fact that there are two components supports our conjecture that at low dopings the material can be characterized by a small FS or electron pocket around $(\pi, 0)$ (volume consistent with $x = 0.04$) with doping-induced spectral weight at higher energy elsewhere in the zone. As the carrier concentration is increased, the $(\pi, 0)$ FS deforms and a new FS segment emerges. It derives from the diagonal feature progressively moving to E_F, as seen by comparing the bottom EDCs of Figs. 2(c)–2(e). These two segments connect to form the LDA-like Fermi surface with volume 1.12 ± 0.05.

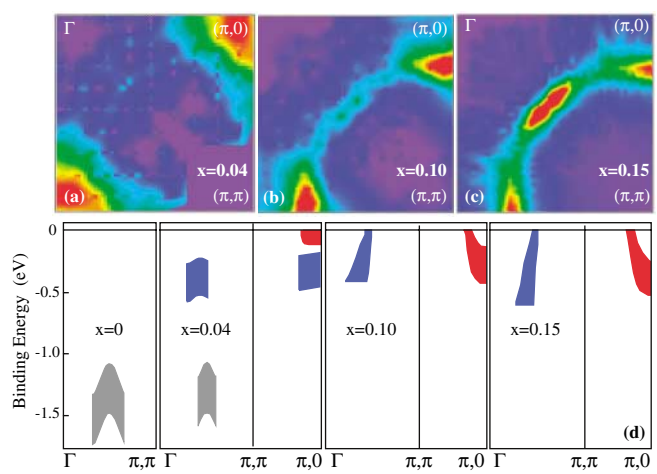

FIG. 3 (color). Fermi surface plots: (a) $x = 0.04$, (b) $x = 0.10$, and (c) $x = 0.15$. EDCs integrated in a 60 meV window (-40 meV, $+20$ meV) plotted as a function of $\vec{k}$. Data were typically taken in the displayed upper octant and symmetrized across the zone diagonal. (d) Panels showing doping dependent "band structure." Features are plotted for the doping levels and momentum space regions where they can be resolved. We do not include the slight low-energy shoulder of the $x = 0$ sample, as this is probably reflective of a small intrinsic doping level.

In the lower panels of Fig. 3, we present a schematic that shows the above described evolution of the E vs $\vec{k}$ relation along two symmetry directions $\Gamma - (\pi, \pi)$ and $(\pi, \pi) - (\pi, 0)$ for the four doping levels. The centroid and widths of the features are plotted for the doping levels and momentum space regions where they can be resolved.

The existence of a Fermi patch at $(\pi, 0)$ in the lightly doped $x = 0.04$ sample is consistent with some calculations based on the $t - t' - t'' - U$ model that predict that the lowest electron-addition states for the $x = 0$ insulator are near $(\pi, 0)$ [18]. This confirms an electron-hole asymmetry (broken by the higher order hopping terms) [18,19] as the lowest hole-addition states for the insulator are near $(\pi/2, \pi/2)$ [3,4,19], and it is the first direct evidence for an indirect CT gap in the cuprates. However, the spectral weight that appears in the CT gap is not explained within a simple LHB/UHB picture. Exact $t - t' - t'' - U$ model numerical calculations have shown evidence for intrinsic excitations to lie in the insulator's gap at low doping [18]. These calculations show the features to have only low spectral weight with the majority contribution at $(\pi, 0)$, as is observed. In addition, the detailed evolution of the electronic structure with doping, especially the $\vec{k}$ space mapping of the low lying excitations of Fig. 3, bears clear resemblance to models that allow the effective U to decrease with doping [20]. Within these models, the CT gap closes with increasing doping and the Fermi level now cuts not only the bottom of the conduction band near $(\pi, 0)$, but also the top of the valence band near $(\pi/2, \pi/2)$ because of the indirect gap [20]. Here, the band structure changes as the antiferromagnetic coherence factors and gap subside.

Starting from the metallic side, an alternative approach may be one that emphasizes a coupling of electrons to magnetic (or similar) fluctuations with characteristic wave vector (π, π). For example, within this picture, as the antiferromagnetic phase is approached and antiferromagnetic correlations become stronger, the "hot spot" regions (intersection of the FS and antiferromagnetic Brillouin zone boundary [14]) may spread so that the zone-diagonal spectral weight is gapped by the approximate nesting of the $(\pi/2, \pi/2)$ section of FS with the $(-\pi/2, -\pi/2)$ section of FS. This scheme obviously breaks down as one gets close to the Mott state, where the zone-diagonal spectral weight is not only gapped, but it also vanishes.

Our finding of an electron pocket that evolves with doping into a large holelike Fermi surface provides a route towards explaining the long-standing puzzle that while transport in these materials exhibits unambiguous n-type carrier behavior at low doping, one has to invoke both electron and hole carriers to explain data near optimal doping [21].

In conclusion, it appears that certain elements of both scenarios presented in the introduction can explain our data. At low carrier concentrations, electrons are doped into regions close to $(\pi, 0)$ (confirming a particle-hole asymmetry), near the energy expected for the UHB forming a small Fermi surface. Simultaneously, there is an appearance of spectral weight at higher energy that begins to span and fill the insulator's gap. At higher electron doping levels, more spectral weight is created in this midgap region and it is this high-energy spectral weight that moves to the chemical potential and completes the $\vec{k}_F$ segment to form a large Fermi surface with a volume close to the expected Luttinger volume.

The authors thank T. Tohyama, P. G. Steeneken, C. Kusko, and R. S. Markiewicz for valuable correspondences. Experimental data were recorded at SSRL which is operated by the DOE Office of Basic Energy Science, Divisions of Chemical Sciences and Material Sciences. Additional support comes from the Office of Naval Research. The crystal growth work at Tokyo was supported in part by Grant-in-Aids for Scientific Research from the Ministry of Education, Science, Sports, and Culture, Japan, and NEDO. The Stanford crystal growth was supported by the U.S. Department of Energy under Contracts No. DE-FG03-99ER45773 and No. DE-AC03-76SF00515, by NSF CAREER Award No. DMR-9985067, and by the A. P. Sloan Foundation.

[1] P. W. Anderson and R. Schrieffer, Phys. Today **44**, No. 6, 54–61 (1991).
[2] J. Zaanen, G. A. Sawatzky, and J. W. Allen, Phys. Rev. Lett. **55**, 418 (1985).
[3] B. O. Wells *et al.,* Phys. Rev. Lett. **74**, 964 (1995).
[4] F. Ronning *et al.,* Science **282**, 2067 (1998).
[5] O. Gunnarsson, O. Jepsen, and Z.-X. Shen, Phys. Rev. B **42**, 8707 (1990).
[6] N. P. Armitage *et al.* (to be published).
[7] M. Meinders, H. Eskes, and G. A. Sawatzky, Phys. Rev. B **48**, 3916 (1993).
[8] J. W. Allen *et al.,* Phys. Rev. Lett. **64**, 595 (1990).
[9] A. Ino *et al.,* Phys. Rev. B **62**, 4137 (2000).
[10] M. A. van Veenedal and G. A. Sawatsky, Phys. Rev. B **49**, 1407 (1994).
[11] Z.-X. Shen and D. Dessau, Phys. Rep. **253**, 2 (1995).
[12] A. Damascelli, D. H. Lu, and Z.-X. Shen, J. Electron Spectrosc. Relat. Phenom. **117–118**, 165–187 (2001).
[13] D. King *et al.,* Phys. Rev. Lett. **70**, 3159 (1993); R. O. Anderson *et al.,* Phys. Rev. Lett. **70**, 3163 (1993); T. Sato, T. Kamiyama, T. Takahashi, K. Kurahashi, and K. Yamada, Science **291**, 1517–1519 (2001).
[14] N. P. Armitage *et al.,* Phys. Rev. Lett. **87**, 147003 (2001).
[15] N. P. Armitage *et al.,* Phys. Rev. Lett. **86**, 1126 (2001).
[16] T. Arima *et al.,* Phys. Rev. B **44**, 917 (1991).
[17] N. Harima *et al.,* Phys. Rev. B **64**, 220507 (2001).
[18] T. Tohyama and S. Maekawa, Phys. Rev. B **64**, 212505 (2001).
[19] C. Kim *et al.,* Phys. Rev. Lett. **80**, 4245 (1998).
[20] C. Kusko, M. Lindroos, A. Bansil, and R. S. Markiewicz, cond-mat/0201117.
[21] Z. Wang *et al.,* Phys. Rev. B **43**, 3020 (1991); S. Kubo and M. Suzuki, Physica (Amsterdam) **185C–189C**, 1251–1252 (1991); W. Jiang *et al.,* Phys. Rev. Lett. **73**, 1291 (1994).